HAL
open science

Podosome rings generate forces that drive saltatory osteoclast migration.

Shiqiong Hu, Emmanuelle Planus, Dan Georgess, Christophe Place, Xianghui Wang, Corinne Albiges-Rizo, Pierre Jurdic, Jean-Christophe Géminard

To cite this version:

Shiqiong Hu, Emmanuelle Planus, Dan Georgess, Christophe Place, Xianghui Wang, et al.. Podosome rings generate forces that drive saltatory osteoclast migration.. Molecular Biology of the Cell, 2011, 22 (17), pp.3120-6. 10.1091/mbc.E11-01-0086 . hal-00603184

HAL Id: hal-00603184

https://hal.science/hal-00603184v1

Submitted on 24 Jun 2011

HAL is a multi-disciplinary open access archive for the deposit and dissemination of scientific research documents, whether they are published or not. The documents may come from teaching and research institutions in France or abroad, or from public or private research centers.

L'archive ouverte pluridisciplinaire **HAL**, est destinée au dépôt et à la diffusion de documents scientifiques de niveau recherche, publiés ou non, émanant des établissements d'enseignement et de recherche français ou étrangers, des laboratoires publics ou privés.

Podosome rings generate forces that drive saltatory osteoclast migration.

Authors:
HU Shiqiong[†,‡], PLANUS Emmanuelle[§], GEORGESS Dan[#], PLACE Christophe[†,‖], WANG Xianghui[‡], ALBIGES-RIZO Corinne[§], JURDIC Pierre[#,*] and GÉMINARD Jean-Christophe[†,*].

Institutions:
[†] Laboratoire de Physique, Ecole Normale Supérieure de Lyon, CNRS, UMR 5672, Lyon, France.
[‡] State Key Laboratory of Precision Spectroscopy, Department of Physics, East China Normal University, Shanghai, China.
[§] Institut Albert Bonniot, Université de Grenoble, Centre de Recherche INSERM-UJF U823, Equipe 1 DySAD - CNRS ERL 5284, Grenoble, France.
[#] Institut de Génomique Fonctionnelle de Lyon, Université de Lyon, UMS 3444 Biosciences Gerland-Lyon Sud, France.
[‖] Laboratoire Joliot-Curie, Ecole Normale Supérieure de Lyon, CNRS, USR 3010, Lyon, France
* Co-last authors

Corresponding author:
Jean-Christophe Géminard,
Laboratoire de Physique, Ecole Normale Supérieure de Lyon,
46, Allée d'Italie, 69364 Lyon cedex 07
Phone/fax : +33 4 72 72 8375/8080
E-mail : Jean-Christophe.Geminard@ens-lyon.fr

Condensed title:
Podosomes drive osteoclast migration.

Character count: 42174

Abstract

Podosomes are dynamic actin-containing adhesion structures that collectively self-organize as rings. In this study, we first show by observing osteoclasts plated on bead-seeded soft substrates that podosome assemblies, such as rings, are involved in tension forces. During the expansion of a podosome ring, substrate displacement is oriented outwards, suggesting that podosomal structures push the substrate away. To further elucidate the function of forces generated by podosomes, we analyze osteoclast migration. Determining the centers of mass of the whole cell G and of actin P, we demonstrate that osteoclasts migrate by 'jumps' and that the trajectories of G and P are strongly correlated. The velocity of the center of mass as a function of time reveals that osteoclasts rapidly catch up with podosomal structures in a periodic pattern. We conclude that actin dynamics inside the cell is not only correlated with cell migration, but drives it.

Introduction

Podosomes are structures, mainly made of actin, found in the contact region between cells and solid substrates. They consist of a dense polymerized-actin core surrounded by a cloud, a loose polymerized actin meshwork (Destaing et al., 2003). Numerous proteins, such as actin regulators or focal adhesion proteins, are associated with these actin structures (Linder, 2009). Podosomes are typically formed in monocyte-derived cells (osteoclasts, macrophages, dendritic cells), endothelial cells and smooth muscle cells. Studies of their molecular components have related them to invadopodia which are mostly found in highly metastatic cancer cells. Even though there are some differences between these two actin-containing structures, they are very similar and often referred to as invadosomes (Linder, 2009).

The main functions of invadosomes are considered to be cell adhesion and matrix degradation. They establish close contact with the substrate and their formation requires integrins (Destaing *et al.*, 2010; Destaing et al., 2011). Indeed, Total Internal Reflection Fluorescence (TIRF) microscopy has shown that podosomes are enriched in adhesion-mediating integrins and form only on the substrate-bound side of the cell (Linder and Aepfelbacher, 2003). Furthermore, there is increasing evidence showing the ability of invadosomes to degrade extracellular matrix (Saltel *et al.*, 2008; West *et al*, 2008, Linder, 2009). It has been recently proven that the invadosome-like structures of lymphocytes are involved in transcellular diapedesis, which has lead to suggest that these structures could probe the endothelial cell surface to allow invasion (Carman, 2009; Carman *et al.*, 2007). Finally, podosomes are thought to play a role in cell migration and invasion, by establishing localized anchorage, stabilizing sites of cell protrusion and enabling directional movement (Linder and Kopp, 2005). However, there is no direct evidence proving the latter mechanism and the role played by the podosomes in cell migration is still unknown.

Osteoclasts, the bone resorbing cells, are large multinucleated hematopoietic cells which exhibit podosomes when adherent, for instance, on plastic or glass. We have previously shown that in osteoclasts, podosomes can collectively self-assemble. They can aggregate in clusters which later form rings. In a transient regime, the rings grow before they dissociate. Podosome rings eventually end up forming belts at the periphery of mature osteoclasts at rest. These belts require an intact microtubule network (Destaing *et al.*, 2003; Destaing *et al.*, 2005), contrary to clusters and rings that are microtubule independent. When adherent on a mineralized extracellular matrix, osteoclasts polarize and podosomes condense to form a large sealing zone delineating the resorption area (Luxenburg *et al.*, 2007; Saltel *et al.*, 2010). This dynamic patterning of podosomes in osteoclasts has been recently shown to depend on the topography of the substrate (Geblinger *et al.*, 2010). These latter data correlate well with previously

described results which have provided the first evidence that invadosomes in rosettes, found in either NIH3T3 fibroblasts or src-transformed BHK cells, are major sites through which cells sense mechanical forces and exert traction forces (Collin *et al.*, 2008; Collin *et al.*, 2006). Nonetheless, the molecular mechanisms governing these forces remain unknown (Destaing *et al.*, 2003; Saltel *et al.*, 2004).

In this study, we describe a series of experiments to elucidate the role played by podosomes in the spreading, migration and retraction of osteoclasts. On one hand, we report observations of actin structures at a short time scale: we describe the spatial organization of podosomes during early adhesion and retraction. In addition, we report the evolution of the 3D shape of an osteoclast in relation with the organization of podosomes in the contact region between the cell membrane and the substrate. We also qualitatively characterize the force applied by the osteoclast onto the substrate. On the other hand, we report a study of the migration process of a single osteoclast at a long time scale, and investigate how the motion of the cell is related to the collective organization of actin. The whole set of experimental results makes it possible to discuss the role of the podosomal structures in osteoclast motility and adhesion process.

Results

Podosomes are involved in maintaining tension in osteoclasts

To further characterize the role of podosomes in osteoclast adhesion, we first observed their behavior during spreading and, inversely, detachment. We used a RAW macrophage cell line stably expressing actin fused to GFP (Destaing *et al.*, 2003) and differentiated into osteoclasts in presence of the two cytokines M-CSF and RANK-L. In a first experiment, we observed the dynamics of the GFP-actin during the early adhesion process: mature osteoclasts were detached and then seeded on glass. The experiment consisted of observing the attachment and spreading by Normarsky contrast and fluorescent time-lapse microscopy (Figure 1A and supplemental movie 1). We observed that the osteoclast, which was initially round before adhering, rapidly spread by forming membrane protusions, reminiscent of corollas, around the central part of the cell. Simultaneously, GFP-actin, which was initially scattered throughout the cell, concentrated at the periphery of the spreading areas and started forming, within 12 minutes of seeding, clearly recognizable podosomes marked by dense actin cores. Additional immunofluorescence staining of actin and vinculin, a podosome cloud component, confirmed that during the first 10 minutes after seeding, the osteoclast is adherent but does not make podosomes: actin is loosely distributed in the cytoplasm and vinculin localizes at the periphery of the cell but does not participate in any organized structures. However, when the osteoclast starts spreading, typical podosomes with F-actin cores and vinculin-containing clouds start to form (Figure 1B). These observations thus revealed that a reorganization of actin results from or drives the spreading process. In a second experiment, adherent osteoclasts were slowly detached by EDTA treatment. We observed that membrane retraction occurred right after the disappearance of podosomes (Figure 1C and supplemental movie 2). Indeed, within two minutes of EDTA treatment all the podosomes dismantled whereas osteoclasts retracted slowly but remained adherent. From these observations, we concluded that the podosomes are not strictly necessary for osteoclast adhesion, but rather play a role in exerting tensions needed for spreading.

The expansion of a podosome ring induces cell displacement

To further figure out the interaction between actin dynamics and osteoclast migratory behaviour, we assessed the 3D shape of an osteoclast vis-à-vis the organization of actin in the contact region between the cell and the substrate. As an osteoclast migrated on a glass dish, we used confocal time-lapse microscopy to image *z*-planes every 15 minutes. Then, *z*-stacks were used to reconstruct the 3D shape of the cell based on fluorescence signal from G-actin diffusing ubiquituously in the cytoplasm (Figure 2 and supplemental movie 3). These observations revealed that the growth of a podosome ring in the contact region is associated with a rapid flattening and migration of the cell.

Again, the dynamics of the actin structure inside the cell is proven to be strongly correlated with the spreading and migration processes.

Podosome structures exert tension on the substrate

In order to assess the forces exerted by an adherent osteoclast, we observed the deformation of the substrate induced by the cell. To do so, we used a soft polyacrylamide gel (stiffness of 0,5 kPa) coated with vitronectin to allow adhesion (Figure 3). The experiment revealed that the displacement of the fluorescent beads in the gel is concentrated around the podosome ring whereas no displacement was ever observed in the regions devoid of podosomes (Figure 3A). Furthermore, when the podosome ring grew and spread, the substrate displacement was mainly oriented outward of the ring (Figure 3B, white arrows). Thus, the podosome ring is subjected to an internal tension which tends to increase its perimeter and, thus, to extend the ring towards the periphery (negative tension). As a consequence, the substrate exerts a compressive force and hence tends to reduce the size of the ring. To conclude, the podosome ring is clearly associated with a tensional effect that tends to stretch the cellular membrane.

Podosome ring expansion drives osteoclast migration

To comprehend the role played by podosome rings in cell motility, we observed the motion of several mature osteoclasts, expressing GFP-actin, seeded on a vitronectin-coated soft polyacrylamide gel (stiffness 3kPa. We chose to work with the same substrate as the one used for the force measurement to get the whole set of experiments in similar conditions). Images were obtained, using time-lapse microscopy, every 5 minutes for about 8 hours (Figure 4 and supplemental movie 4). Qualitatively, in the whole set of experiments (4 mature osteoclasts on polyacrylamide gel), we observed that the cell migrates randomly. More precisely, the formation of podosome rings inside the osteoclast accompanies its elongation in one given direction. When the maximal length L of the cell is about twice its typical size, the actin structure disappears from one side and the cell retracts towards the remaining structure on the opposite side which becomes the leading edge (Figure 4, $t = 120$ min). This results in a 'jump' of the cell in the corresponding direction (Figure 4, $t = 150-180$ min). Subsequently, the cell elongates in an almost perpendicular direction due to the growth of two new rings from the remaining structure at the leading edge (Figure 4, $t = 210$ min). Below, we report a representative quantitative study of the cell motion.

In a first step, it is particularly interesting to focus on the dynamics of the cell's center of mass, G (*see* Materials and Methods). We reported the trajectory of G in the sample plane (X, Y) during the whole experimental time (Figure 4, bottom-right and Figure 5). The first striking result is that the cell moves in a series of straight jumps separated by spatially localized changes in direction. In order to get information about the dynamics,

we reported the velocity of the center of mass, V_G, as a function of time t (Figure 6A) and noticed that V_G exhibits large peaks (A to D) almost periodically every 2 hours.

Then, in order to account for the potential coupling between the motility of the cell, characterized by the motion of the center of mass G, and the internal dynamics of actin, we defined a point P, summarizing the position of all actin inside the cell (*see* Materials and Methods). We also defined the vector $\vec{f} \equiv \overrightarrow{GP}$ which accounts for the distance and direction between the center of mass G and the location of actin P (Figure 4). Reporting the trajectory of P in the (X, Y) plane (Figure 5), we observed first that G and P experience the same trajectories. To provide information about the dynamics, we reported the distance $f \equiv \|\overrightarrow{GP}\|$ between G and P as a function of time t (Figure 6B). We then observed that f and V_G are also strongly correlated in time, a large peak in f preceding each large peak in V_G. The temporal correlation between f and V_G and especially the delay τ between the peak in f and the peak in V_G can be assessed by calculating the cross-correlation function $\chi(t) \equiv \int f(t' - t) V_G(t') dt$, where the integral is estimated over the whole experimental time (Figure 7). The experimental correlation function $\chi(t)$ exhibited a maximum for $t \equiv \tau = 10$ minutes whereas the oscillations pointed out the period of the cell motion, $T \approx 2$ hours. In the same way, we reported the cell length L as a function of time t (Figure 6C). We observed that the cell length L increased almost linearly between two successive jumps. The disappearance of one of the actin structures on one side leads to a peak in f when L is maximum (Figure 6B).

We considered the direction of the jumps by identifying first the peaks A, B, C and D, as defined in the figure 6, and the associated minima in the velocity (numbered from 1 to 5 such that the peak A is associated to the jump from G_1 to G_2, etc). On the one hand, we denoted $\overrightarrow{f_A}$, $\overrightarrow{f_B}$, $\overrightarrow{f_C}$ and $\overrightarrow{f_D}$, the values of $\vec{f}$ at the peaks A, B, C and D. On the other hand, we denoted $\overrightarrow{\Delta G_{ij}} \equiv \overrightarrow{G_i G_j}$, the vector associated to the displacement of G during the jumps from i to j. Reporting the values of $\vec{f}$ at the maxima and the corresponding displacements $\overrightarrow{\Delta G}$, we observed that these quantities are correlated in both length and direction (Figure 8). First, the angles θ_P and θ_G that $\vec{f}$ and $\overrightarrow{\Delta G}$ make with the X-axis are equal (Figure 8A), which proves that the jumps occur in the direction of $\vec{f}$. Second, the amplitude ΔG of the jumps is proportional to f (or, equivalently, to L) (Figure 8B). Finally, note that the successive jumps occur in directions making angles of about 90 degrees between them (Figure 8).

As a conclusion of this last experiment, the osteoclast *'jumps'* follow the internal organization of actin. We insist here that the point P refers to all G-actin monomers in the cell, including the ones present in structures made of F-actin polymers. We show that the growth of rings induces the elongation of the cell. When the length L of the cell in a given direction is about twice its initial size before expansion, one of the actin rings takes the lead at one end whereas the others disassemble. Subsequently the cell retracts

toward the remaining structures, which leads to a *'jump'* of the cell in the given direction about 10 minutes after f (or L) has reached a maximum. The process repeats itself almost periodically every two hours. Thus, the motion of the cell occurs by seemingly periodic jumps, the length of which is about the cell size, during which the cell moves rapidly in a given direction resulting in saltatory migration.

Discussion

We have investigated the role played by podosomes in the migratory behavior of osteoclasts. In summary, podosome rings exert tension forces, tending to extend the cellular membrane and pushing the substrate outwards. Podosome assemblies, even if being in close contact with the substrate, do not play a direct role in cell adhesion; rather they exert forces where tension is needed, forming in expanding regions and disappearing from retracting regions. Discussing in detail the migration of a set of osteoclasts from a RAW monocytic cell line expressing an actin green fluorescent protein, we showed that osteoclasts move by '*jumps*', rapidly catching up with podosomal structrures in a periodic pattern.

One could wonder if our experimental observations are not too specific and correspond to a general pattern. First, we can state that all the RAW-derived osteoclasts we observed were exhibiting qualitatively the same type of motion as proven by cells exhibiting mainly two or more podosome rings and even podosome clusters (supplemental movie 5). Second, in order to confirm results with different substrate and osteoclast origins, we studied in addition the dynamics of primary osteoclasts expressing LifeAct-eGFP moving on glass. We observed the exact same migration pattern (supplemental data 6 and movie 6). These experiments demonstrate that the observed pattern is not specific of the RAW cell line and substrate (vitronectin-coated polyacrylamide) and that the dynamics of actin inside the osteoclast are not only correlated with cell migration, but drive it.

At this point, we can propose a potential mechanism which can account for the osteoclast migration. The migration of osteoclasts involves their elongation which is correlated with the growth of podosome rings. Podosomes collectively push the cell membrane outwards as already observed during the early spreading process. From the observation of substrate displacement, we concluded, in agreement with previous investigations on BHK-RSV cells showing torsional tractions underneath the podosome rings (Collin *et al.*, 2008), that podosome rings exert forces onto the substrate. As the associated substrate displacement points outwards, we propose that the ring is subjected to an internal tension which tends to extend it. Thus, the formation and growth of a podosome ring can account for the spreading of the contact region. Indeed, a podosome ring that encounters the cell periphery pushes the membrane outwards. The process can take place until the membrane has reached its maximal possible extension (the cell is then flat). If two rings are pushing the cell in two opposite directions, the cell length increases until the weakest ring loses its mechanical stability because of excessive stress. Then, the weaker disappears and the cell jumps in the direction of the remaining.

Last, we discuss the physical origin of the tension force. Individual podosomes are associated with a dense actin core formed by the cross-linked actin filaments, as

demonstrated by SEM observation experiments (Luxenburg *et al.*, 2007). We have previously proposed that actin cores have a conical shape (Destaing *et al.*, 2003; Jurdic *et al.*, 2006; Hu *et al.*, 2011); they are dynamical structures growing from the the cell membrane, at the substrate interface, and dissociating from the top (Figure 9A). Considering the sketch in the figure 9B, one can easily see that, because of a steric frustration effect, the base of the cone tends to extend if the structure grows from the base and the filaments are linked to each other. As a consequence, two neighboring podosomes tend to repel each other, which naturally explains why a ring structure is subjected to an internal tension which tends to increase the length of a podosome line (negative tension) and, accordingly, the ring diameter. In such a picture, the podosomes are thus responsible for the membrane tension. What remains unexplained are the molecular mechanisms involved in the transmission of the tension from the membrane to the substrate at the podosome base.

The mechanism that we propose is based on several assumptions (for instance, the cell adheres to the substrate in the contact region and the podosomal structure becomes unstable when the stress is released) but it is compatible with the seemingly periodic movement of the cell in the direction of $\overrightarrow{GP}$, thus toward the actin structure. First, as explained above, the cell moves in the direction of $\overrightarrow{GP}$. One can estimate the growth velocity of the ring from the period T, which corresponds to the time needed for two rings to push the cell membrane over a distance that compares to the cell size. From the slope dL/dt (Figure 6C), we have estimated that the ring growth-velocity is of the order of $v \approx 0{,}25$ µm/min (L increases by about 50 µm in 100 min due to the action of two rings). From the growth velocity v, taking into account the typical distance between two podosomes which is of about 1 µm, we estimate that the typical lifespan of one podosome is of about 4 min. The latter estimate agrees reasonably with previous results (Destaing *et al.*, 2003; Geblinger *et al.*, 2010), which again sustains our model. Second, it is interesting to note that the assumption that the podosomal structure becomes unstable when the stress is released would be compatible with the fact that successive jumps make a 90 degree angle between them, at least when two rings develop in opposite directions. Indeed, when the cell reaches its maximal elongation, the disappearance of one of the podosomal structures releases the stress along $\vec{f}$. As a consequence, the remaining podosomal structure becomes unstable along $\vec{f}$. This instability could explain why two secondary rings, aligned in a perpendicular direction, form and grow from the remaining ring.

The saltatory migration of osteoclasts described here is reminiscent of the saltatory migration of oligodendrocyte precursors dispersing from the ventricular zone during the early brain development and described as alternating stationary and fast-moving phases (Tsai *et al.*, 2009). It could reflect the inchworm like progression of bone resorbing osteoclasts that we have described earlier (Saltel *et al.*, 2004).

Materials and Methods

◦ *Osteoclast differentiation:*

To image podosomes in osteoclasts, we have used the RAW monocytic cell line expressing an actin green fluorescent protein (GFP) (Destaing et al., 2003). The RAW 264.7 cells, from American Type Culture Collection (Manassas, VA), were transfected in our lab with FuGENE 6 following manufacturer's recommendations (Roche Diagnostics). Then, the cells were regularly selected by flow cytometry (FACScan) to maintain a stable RAW cell line expressing GFP-actin. The GFP-actin RAW cells were cultured with a density of about 50 cells/mm^2 in a 12 wells plate for 6 days in order that they differentiated into osteoclasts. Primary murine osteoclasts were differentiated from the bone marrow of 8 week-old mice as described in Destaing *et al*, 2003. The differentiation medium was α-minimal essential medium (αMEM, Invitrogen) containing 10 % fetal bovine serum (Bio West, France), 30 ng/ml M-CSF, and 35 ng/mL RANK-L. Recombinant human RANK-L and human M-CSF were produced in our laboratory as previously described (Destaing *et al.*, 2003). Culture medium was changed every two days. After 6 days of differentiation, mature osteoclasts were washed twice with PBS and detached by using 0.25 µM EDTA in PBS for 5 minutes (EDTA chelates divalent ions that are essential to activate membrane receptors involved in the cell adhesion). After centrifugation, osteoclasts were seeded with a density of about 100 cells/mm^2, either on a glass bottom dish (MatTeK, USA) or on a polyacrylamide gel.

◦ *Transient transfection*:

For videomicroscopy of the actin cytoskeleton in primary osteoclasts, day 4 osteoclasts were transfected with pEGFP-N1-LifeAct (Riedl *et al*, 2008) using Lipofectamine™ LTX with PLUS™ Reagent (Life Technologies) following the manufacturer's instructions. After 48 hours, cells were detached using EDTA and replated on a glass bottom dish as mentioned previously.

◦ *Indirect immunofluorescence*:

To observe podosome formation during spreading, osteoclasts derived from RAW 264.7 cells were reseeded on a glass bottom dish as mentioned earlier. Briefly, cells were fixed with 4% paraformaldehyde (pH 7.2) at 10 minutes and 25 minutes after re-seeding. They were permeabilized with 0.2% Triton-X-100® in PBS and then incubated for 1h with anti-Vinculin antibody (Clone hVIN1, #V9264, Sigma) at 10 µg/mL final concentration. Cells were then washed 3 times with PBS and incubated with Alexa Fluor® 488 Phalloidin (Life Sciences) and Alexa Fluor® 647 Goat anti-Mouse IgG (A21236, Life Sciences) at 2 µg/mL for 45 minutes. Samples were washed and kept in PBS for microscopy.

◦ *Confocal microscopy:*
Living cells were imaged in an inverted microscope (Leica DMI 4000) equipped with a confocal spinning-disk unit (Yokogawa CUS22) and an incubating chamber at 37°C with 5% CO_2 and humidity-saturated atmosphere. The light source consisted of a laser diode (excitation wavelength 491 nm and 647 nm, Roper Scientific) and we used an emission filter with a 500-550 nm or 641-708 nm bandpass (Semrock). For timelapse microscopy, we recorded, during 8 hours, one image from a QuantEM camera (Photometric) every 5 minutes using a 20x objective. For fixed samples, we used a 100x oil immersion objective.

◦ *Soft gel substrate:*
Polyacrylamide gels were prepared at the bottom surface (diameter 14 mm) of glass bottom dishes (MatTeK, USA). First, the glass bottom surface of the MatTek culture dishes were pretreated with 500 µL Bind-Silane (g methacryloxypropyltrimethoxy-silane, GE life science) by applying the solution with a cotton swap and, then, drying the surface under a hood. At the same time, glass coverslips (diameters 12 mm) were quickly treated with 15 µL Sigmacote (Sigma) and then also dried under the hood.

Polyacrylamide gels exhibiting two different rigidities were obtained, according to the ratio 8% acrylamide/0.05% bis-acrylamide for a very soft gel (stiffness 0,5kPa) or the ratio 8% acrylamide/0.1% bis-acrylamide for a soft gel (stiffness 3kPa). Fluorescent beads (diameters 210 nm; Invitrogen™ Molecular Probes™) were seeded in the softer gel. 2.5 ml solution was obtained by mixing 500 µL acrylamide 40%, 62.5 µL bisacrylamide 2%, 25 µL Hepes 1M pH 8.5, 80 µL 2% beads solution and water. Then, 12.5 µL ammonium persulfate and 1.25 µL TEMED were added to allow polymerization. The final solution (8 µL) was dropped on a Bind-Silane treated MatTek dish coverslip which was then covered by a Sigmacote treated coverslip. After 20 min of polymerization, the upper coverslip was removed.

Finally, the gel surface was activated with vitronectin (BD Biosciences) as described by Damljanovic *et al.* (2005). Briefly, pure hydrazine hydrate (Sigma) was added on the gels for 2 h, then gels were washed with 5 % glacial acetic acid for 1 h, followed by distilled water for 1 h. Vitronectin solution (10 µg/ml) was diluted in 50 mM sodium acetate buffer at pH 4. The oxidation of vitronectin was achieved by adding 3.6 mg/ml sodium periodate crystals (Sigma) and incubation at room temperature for 30 min. Oxidized vitronectin (150 µL) was added on the polyacrylamide treated gel and incubated at room temperature for 1 h, then washed with PBS.

◦*Analysis of the substrate displacement field:*
We used the open software package JPIV for Particle Image Velocimetry (PIV) (www.jpiv.vennemann-online.de/) to determine the displacements of the fluorescent beads in the (X, Y) plane with respect to their initial positions.

◦ *Cell tracking image analysis:*

Stacks of images and associated data were analyzed using the image processing and analysis software ImageJ (http://rsb.info.nih.gov/ij/) and the technical graphing and data analysis software *Igor Pro* (WaveMetrics, Inc.). We denoted M and N, the dimensions in pixels of the image in the directions m and n, respectively. We determined:

the position (m_G, n_G) of the **center of mass** of a cell, G:

From one raw fluorescence image I_{mn}, using an intensity threshold, we obtained a binary image B_{mn} of the cell such that $B_{mn} = 1$ if the indices m and n correspond to a point inside the cell and $B_{mn} = 0$ otherwise. By definition, $m_G \equiv \frac{1}{NM}\sum_{n=1}^{N}\sum_{m=1}^{M} m.B_{mn}$ and $n_G \equiv \frac{1}{NM}\sum_{n=1}^{N}\sum_{m=1}^{M} n.B_{mn}$.

the position (m_P, n_P) of **actin**, P:

In order to obtain a point P which characterizes the position of actin inside the cell, from one raw fluorescence image, we defined$m_P \equiv \frac{1}{NM}\sum_{n=1}^{N}\sum_{m=1}^{M} m.I_{mn}^{\alpha}$, and $n_P \equiv \frac{1}{NM}\sum_{n=1}^{N}\sum_{m=1}^{M} n.I_{mn}^{\alpha}$. We introduced the exponent α in order to increase the contrast. We checked that the experimental results do not depend significantly on α and report results obtained with $\alpha = 3$.

Finally, scaling factors were applied to convert (m_G, n_G) and(m_P, n_P) to the positions (X_G, Y_G) and (X_P, Y_P) in the sample plane (X, Y).

Acknowledgments

We thank C. Chamot and C. Lyonnet from the Imaging Platform (PLATIM) of UMS3444/US8 Biosciences for their precious help and advices; C. Domenget and all members of P. Jurdic's team for their support and assistance in osteoclast cultures; O. Destaing and F. Saltel for Fig. 9A. This work was supported by recurrent grants from CNRS, and ENS Lyon and grants from the Association pour la Recherche sur le Cancer (ARC), the Agence Nationale de la Recherche (« podosomes »), and the Fondation pour la Recherche Médicale (DEQ20051205752). D. Georgess is supported by Marie-Curie actions (FP7, T3Net).

References

Abramoff, M.D., Magelhaes P.J., Ram S.J. (2004). Image Processing with ImageJ. *Biophotonics International.* 11, 36-42.

Carman, C.V. (2009). Mechanisms for transcellular diapedesis: probing and pathfinding by 'invadosome-like protrusions'. *J Cell Sci*. 122, 3025-3035.

Carman, C.V., Sage P.T., Sciuto T.E., de la Fuente M.A., Geha R.S., Ochs H.D., Dvorak H.F., Dvorak A.M., and Springer T.A. (2007). Transcellular diapedesis is initiated by invasive podosomes. *Immunity*. 26, 784-797.

Collin, O., Na S., Chowdhury F., Hong M., Shin M.E., Wang F., and Wang N. (2008). Self-organized podosomes are dynamic mechanosensors. *Curr Biol*. 18, 1288-1294.

Collin, O., Tracqui P., Stephanou A., Usson Y., Clement-Lacroix J., and Planus E. (2006). Spatiotemporal dynamics of actin-rich adhesion microdomains: influence of substrate flexibility. *J Cell Sci*. 119,1914-1925.

Destaing, O., Planus E., Bouvard D., Oddou C., Badowski C., Bossy V., Raducanu A., Fourcade B., Albiges-Rizo C., and Block M.R. (2010). beta1A integrin is a master regulator of invadosome organization and function. *Mol Biol Cell*. 21, 4108-4119.

Destaing O., Block M., Planus E. and Albiges-Rizo C. (2011). Invadsome regulation by adhesion signaling, *Curr. Opin. Cell Biol.* 23, 1-10.

Destaing, O., Saltel F., Geminard J.C., Jurdic P., and Bard F. (2003). Podosomes display actin turnover and dynamic self-organization in osteoclasts expressing actin-green fluorescent protein. *Mol Biol Cell*. 14, 407-416.

Destaing, O., Saltel F., Gilquin B., Chabadel A., Khochbin S., Ory S., and Jurdic P. (2005). A novel Rho-mDia2-HDAC6 pathway controls podosome patterning through microtubule acetylation in osteoclasts. *J Cell Sci*. 118, 2901-2911.

Geblinger, D., Addadi L., and Geiger B. (2010). Nano-topography sensing by osteoclasts. *J Cell Sci*. 123, 1503-1510.

Hu, S., Biben T., Wang X., Jurdic P., and Géminard J.-C. (2011). Internal dynamics of actin structures involved in the cell motility and adhesion: modeling of the podosomes at the molecular level. *J Th. Biol.* 270, 25-30.

Jurdic, P., Saltel F., Chabadel A., and Destaing O. (2006). Podosome and sealing zone: specificity of the osteoclast model. *Eur J Cell Biol*. 85, 195-202.

Linder, S. (2009). Invadosomes at a glance. *J Cell Sci*. 122, 3009-3013.

Linder, S., and Aepfelbacher M. (2003). Podosomes: adhesion hot-spots of invasive cells. *Trends Cell Biol*. 13, 376-385.

Linder, S. and Kopp P. (2005). Podosomes at a glance. *J Cell Sci*. 118, 2079-2082.

Luxenburg, C., Geblinger D., Klein E., Anderson K., Hanein D., Geiger B., and Addadi L. (2007). The architecture of the adhesive apparatus of cultured osteoclasts: from podosome formation to sealing zone assembly. *PLoS One*. 2, e179.

Riedl J. *et al* (2008). Lifeact: a versatile marker to visualize F-actin. *Nature Methods* 5, 605-607.

Saltel, F., Daubon T., Juin A., Ganuza I.E., Veillat V., and Genot E. (2011). Invadosomes: Intriguing structures with promise. *Eur J Cell Biol*. 90, 100-107.
Saltel, F., Chabadel A., Bonnelye E., and Jurdic P. (2008). Actin cytoskeletal organisation in osteoclasts: A model to decipher transmigration and matrix degradation, *Eur. J. Cell Biol.*, 87, 459-468.
Saltel, F., Destaing O., Bard F., Eichert D., and Jurdic P. (2004). Apatite-mediated actin dynamics in resorbing osteoclasts. *Mol Biol Cell*. 15, 5231-5241.
Tsai, H.H., Macklin W.B., and Miller R.H. (2009). Distinct modes of migration position oligodendrocyte precursors for localized cell division in the developing spinal cord. *J Neurosci Res*. 87, 3320-3330.
West, M.A., Prescott A.R., Chan K.M., Zhou Z., Rose-John S., Scheller J., and Watts C. (2008). TLR ligand-induced podosome disassembly in dendritic cells is ADAM17 dependent. *J Cell Biol.* 182, 993-1005.

Abbreviations List

3D: Three-Dimensional
EDTA: Ethylene Diamine Tetraacetic Acid
FACScan: Fluorescence Activated Cell Sorting Scan
GFP: Green Fluorescent Protein
M-CSF: Macrophage-Colony Stimulating Factor
αMEM: α-Minimal Essential Medium
RANK-L: Receptor Activator of Nuclear factor κB -Ligand
SEM: Scanning Electron Microscopy
TEMED: TEtraMEthylethyleneDiamine
TIRF: Total Internal Reflection Fluorescence

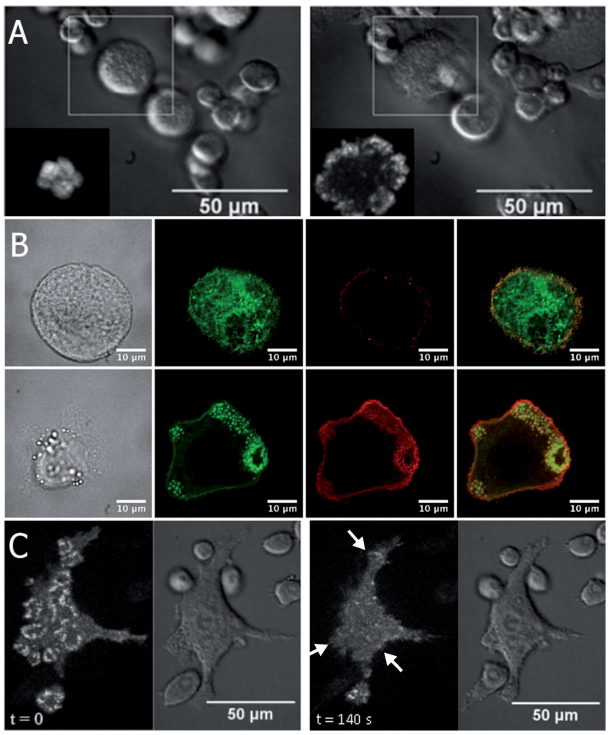

Figure 1. Podosomes are involved in maintaining tension in osteoclasts. (A) During adhesion and spreading processes, the podosomes accumulate along the periphery of the cell, in the expanding regions - Several mature osteoclasts, expressing GFP-actin, are seeded onto a glass coverslip and observed under the microscope using a Nomarski contrast. Insets: Fluorescence image of the cell which is pointed out by the white square. Left panel: 5 minutes after seeding, the cell is round and actin is scattered in the cytoplasm (inset). Right panel: 20 minutes after seeding, the considered cell starts spreading. The fluorescence image (inset) reveals that actin becomes concentrated in podosomes along the periphery of the contact region, where the cell is expanding. (B) Immunofluorescent labelling of adherent osteoclasts spreading on glass: actin stained with Phalloidin (green) and vinculin stained with anti-vinculin (red). Upper pannel: 10 minutes after seeding, actin is loosely distributed in the cytoplasm of the osteoclast and vinculin staining confirms the absence of podosomes. Lower pannel: 25 minutes after seeding, podosomes form where the cell is expanding. Vinculin marks the periphery (surrounding cloud) of the podosomes. (C) Osteoclasts remain adherent even in the absence of podosomes – At $t = 0$ s, the cell is spread, in close contact with the substrate (right) and the fluorescence image (left) reveals several rings of podosomes (bright spots). At $t = 140$ s, the addition of EDTA produced a rapid dissociation of podosomes associated with cell retraction (pointed out by white arrows).

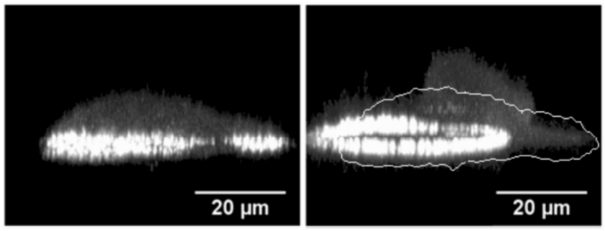

Figure 2. The podosome ring expansion correlates with the direction of migration. One osteoclast expressing the GFP-actin adherent on glass is imaged under confocal microscope. The actin organization in the contact area with the substrate is revealed by slightly tilting the reconstructed images along the Z axis. Left panel: One observes that actin, which concentrates is the base plane, is organized in two rings, the largest located on the left-hand-side. The fluorescence signal from the actin monomers that ubiquituously invade the cytoplasm clearly reveals the shape of the cell. Right panel: 75 minutes later, the largest ring grew and the smallest disappeared. Simultaneously, the cell flattened above the remaining ring, expanded in that regions and, in addition, moved to the left (the white contour corresponds to the initial shape of the cell in the left panel).

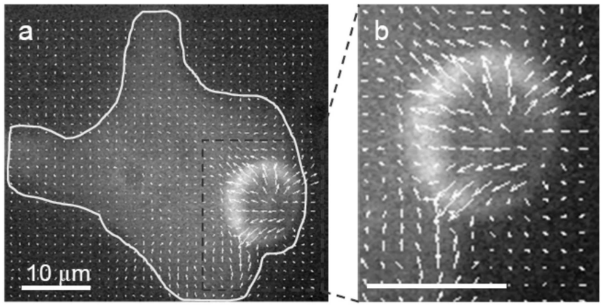

Figure 3. Actin ring structures exert tension forces on the substrate. We observe the dynamics of a live osteoclast, expressing GFP-actin moving on the surface of a soft polyacrylamide gel (stiffness 0,5 kPa). The gel containing fluorescent beads (rhodamine, diameter 210 nm) is coated with vitronectin. Images of GFP-actin and of the rhodamine beads were taken every minute. The substrate displacement field is reconstructed by tracking the displacements of the fluorescent beads. (A) The merge of the osteoclast image (GFP-actin) and of the displacement field (arrows indicate the local displacement with respect to the substrate at rest) reveals that the displacement is significant solely around the podosomal structure (*ring*). (B) Enlargement of the podosomal structure as delineated by the rectangle in (A). The displacements of the beads clearly reveal that the *ring* pushes the substrate outward.

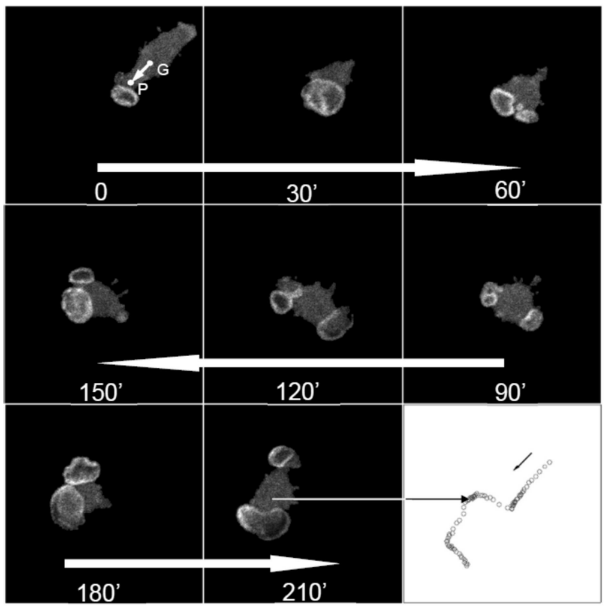

Figure 4. Podosome ring expansion and osteoclast migration are correlated. Using time-lapse fluorescence microscopy, we observe the dynamics of an osteoclast expressing GFP-actin moving on the surface of a polyacrylamide gel (stiffness 3 kPa, supplemental movie 4). Here, we report 8 successive images separated by 30 minutes. From such images, we determined (see Materials and Methods) the center of mass of the cell G, the position of the actin structure P, and defined the vector $\vec{f} \equiv \overrightarrow{GP}$. We report the points G and P for the first image ($t = 0$, top-left). Bottom-right: successive positions, separated by 5 minutes, of the center of mass G determined from this image sequence (same scale).

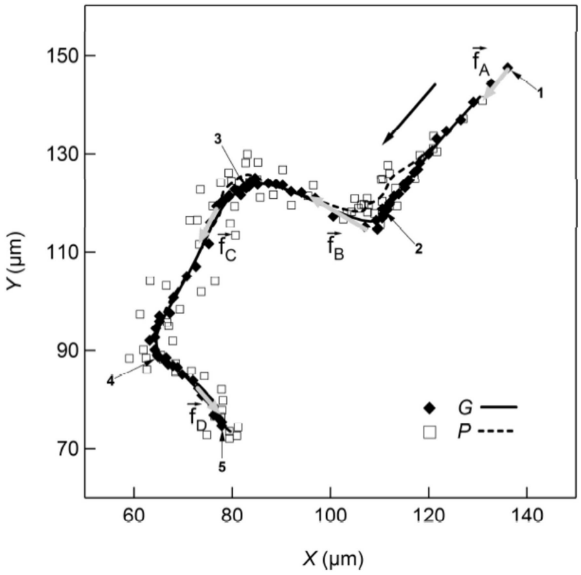

Figure 5. Successive positions of the center of mass, G, and of actin, P, in the sample plane (X, Y). The time difference between two successive points is 5 minutes. The black arrow points the direction of the motion. The continuous and dashed lines correspond to the trajectory of G and P respectively, averaged over 10 successive positions. The trajectories of G (full diamonds) and P (open squares) are strongly correlated. The vectors $\vec{f}_A$, $\vec{f}_B$, $\vec{f}_C$ and $\vec{f}_D$ (grey arrows) are associated to the events A, B, C and D, and the tags 1 to 5 indicate the minima in the velocity V_G, as defined in the figure 6.

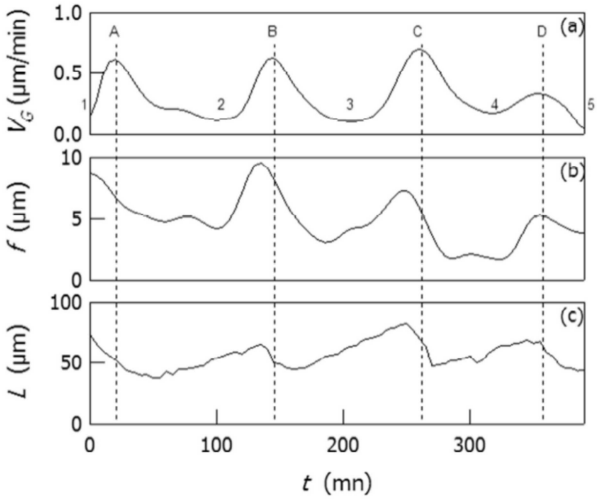

Figure 6. Velocity of the center of mass V_G, distance f and cell length L as a function of time t. (A) The velocity V_G exhibits peaks which correspond to a rapid motion of the cell in a given direction (*jump*). We number from 1 to 5 the minima in the velocity V_G. (B) The distance f interestingly exhibits the same type of temporal evolution. (C) The cell length L increases slowly when the cell velocity is small and rapidly decreases during the jumps. One can notice that the cell *jumps* about 10 minutes after f or L have reached a maximum. We identify here 4 events, *A*, *B*, *C* and *D*. Successive jumps are separated by about 2 hours.

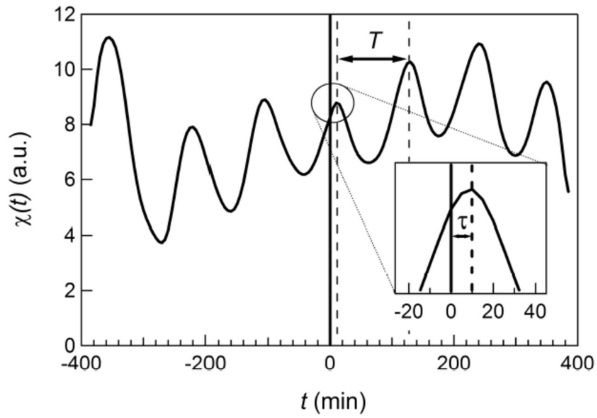

Figure 7. Temporal cross-correlation $\chi(t)$ between the distance f and the cell velocity V_G. The oscillations of the correlation function confirm the almost periodic character of the jumps, with a period $T \approx 2$ hours. *Inset:* Enlargement of the central peak. The correlation $\chi(t)$ is maximum for $t \equiv \tau \approx 10$ minutes, which shows that the cell jumps about 10 minutes after f has reached a maximum.

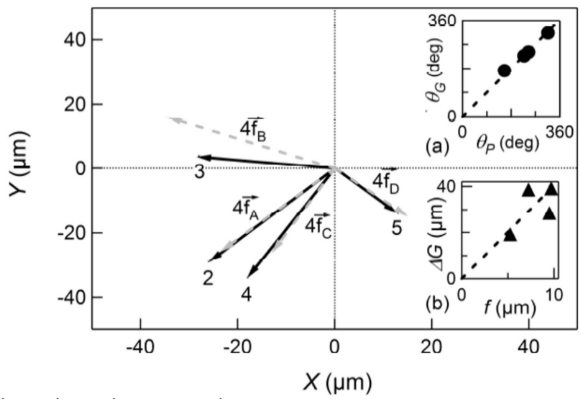

Figure 8. Vectors $\vec{f}_A, \vec{f}_B, \vec{f}_C$ and $\vec{f}_D$ and associated displacements $\overrightarrow{\Delta G}$. The cell center of mass G jumps toward P as pointed out by the strong correlation between $\vec{f}$ at the maximum (grey dotted arrows) and the corresponding $\overrightarrow{\Delta G}$ (black arrows). (A) : Angle θ_G vs. angle θ_P. The dotted line corresponds to the slope 1 showing that $\theta_G \approx \theta_P$. (B) : Jump length ΔG vs. maximum distance f. The cell moves over a larger distance when the distance f at the maximum is larger.

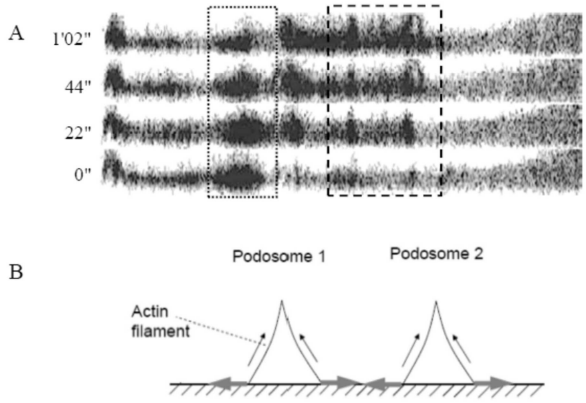

Figure 9. Sketch of forces exerted by two growing podosomes. (A) Podosomes in the contact region between an osteoclast and a plastic dish were imaged under the confocal microscope. Stacks of pictures were then used to reconstitute a Z image, thus the profiles of the podosomes in a vertical plane (Time 0, 22, 44 and 62 seconds). The sequence shows that the podosomes consist of actin filaments which grow rapidly from the cell membrane (thick dotted rectangle on the right) and disappear from the top (dotted rectangle on the left). (B) We have previously proposed that the actin cores of podosomes are organized in a conical brush (Destaing *et al.*, 2003; Jurdic *et al.*, 2006, Hu *et al.*, 2011). Because actin filaments are cross-linked and growing from the membrane, the actin filaments, due to steric constraints, repel each other in the base plane. Thus, two neighboring podosomes tend naturally to repel each other and thus generate the negative tension associated with the podosomal structure. Grey arrows: forces exerted by neighboring podosomes on the substrate.

Supplemental movie 1:
Movie of adhesion, for the figure 1A

Supplemental movie 2:
Movie of detachment, for the figure 1B

Supplemental movie 3:
Movie of 3D-shape of a migrating osteoclast, for the figure 2

Supplemental movie 4:
Movie of osteoclast migration, for the figure 4.
The corresponding trajectories of G and P are reported in the right panel.

Supplemental movie 5:
Additional movie of osteoclast migration, same conditions as in movie 4 with the cell rather exhibiting podosome clusters.

Supplemental movie 6:
Movie of murine bone marrow-derived osteoclast migrating on glass.

Supplemental data 6:
Using time-lapse microscopy as in figure 4, we observe the dynamics of a murine bone marrow-derived osteoclast expressing LifeAct-eGFP moving on glass. We report 8 successive images depicting significant timepoints of migration. From such images, we determined the trajectory of the center of mass G (right bottom).